

AD-A044789



Gulf General Atomic
Incorporated

GA-10002

STUDY OF EFFECTS OF IONIZING RADIATION IN CAPACITORS

FINAL REPORT

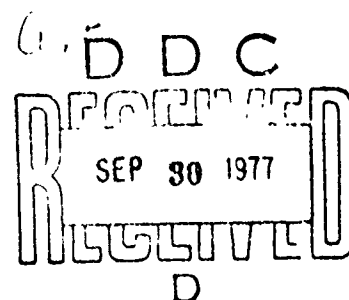
by

T. M. Flanagan and J. W. Harrity

CLEARED
FOR OPEN PUBLICATION

JUL 20 1977
DIRECTORATE FOR FREEDOM OF INFORMATION
AND SECURITY REVIEW (OASD-PA)
DEPARTMENT OF DEFENSE

Prepared under 0114
Contract DASA01-69-C-0014
for the
Department of Defense
Defense Atomic Support Agency
Washington, D. C. 20305



April 20, 1970

ACCESSION for _____	
WTS	White Section X
1.2	But
Per ltr. on file	
A	

Gulf General Atomic

Incorporated

P.O. Box 608, San Diego, California 92112

GA-10002

STUDY OF EFFECTS OF IONIZING RADIATION IN CAPACITORS

FINAL REPORT

by

T. M. Flanagan and J. W. Harrity

Prepared under
Contract DASA01-C-0014
for the
Department of Defense
Defense Atomic Support Agency
Washington, D. C. 20305

DASA 01-69-C-0114

April 20, 1970

DISTRIBUTION STATEMENT A

Approved for public release;

Distribution Unlimited

1. INTRODUCTION

Recent advances in the theory^(1,2) of ionization effects in dielectrics have revealed serious deficiencies in the existing data on radiation effects in capacitor materials. From a circuit applications standpoint, the most important effect of radiation on a capacitor is the induced conductivity in the dielectric material. Most of the data obtained in the past were taken with a view to generating those parameters that characterize a steady-state photoconductivity theory. In this steady-state theory, it was assumed that the duration of the radiation pulse is longer than the duration of the longest delayed conductivity component. This assumption, which automatically eliminates consideration of dose dependences, is not appropriate to most TREE applications. This implies that the fitting parameters obtained for the steady-state formulation from transient experiments do not accurately reflect the physical processes occurring in the dielectric and, thus, cannot be used to understand the mechanisms for the radiation response. Since capacitor response prediction is important to circuit designers, the data used to predict capacitor response should now be updated.

The three stated goals of the present program were:

1. Survey the literature and evaluate the ionizing response of common dielectric capacitors with a view to generating the parameters needed for prediction formulas of the new theories.
2. Perform tests, using 30-MeV electron irradiations, to provide data for obtaining those parameters not obtained from the literature review.
3. Prepare a suggested draft of the capacitor chapter, Section H, of the TREE Handbook.

Since an intensive literature search revealed that very little data have been published which are suitable for generating the needed fitting

parameters, radiation testing of all the relevant capacitor types was deemed necessary. This report presents the results of those tests. A suggested draft for Section H of the TREE Handbook is presented as Appendix A.

2. EXPERIMENTAL AND ANALYTICAL APPROACH

Eleven capacitor types were selected for testing on the Gulf General Atomic (GGA) linear accelerator (Linac). These types, together with pertinent information on the individual capacitors, are listed in Table 1. The value of the capacitance listed under C_{meas} was determined from measurements on a capacitance bridge.

The circuit used in the tests is represented schematically in Fig. 1. Here, C is the capacitor under test, R is the series resistor across which the current in the circuit is measured, E_0 is the impressed charging potential, and $G(t)$ is the radiation-induced conductance of the dielectric of the capacitor. The signal $V(t)$, representing the current in the circuit, appears as in Fig. 2a or Fig. 2b, depending on the circuit time constant.

If the RC charging time of the circuit is much less than the radiation pulse width t_p , the current signal of Fig. 2a, which closely follows the actual shape of the induced conductance, is obtained. When RC is long compared to the pulse width, a signal resembling Fig. 2b is observed: a steady rise during the pulse, followed by a slower rise immediately after the pulse corresponding to a continuing discharge of the capacitor due to the delayed conductivity components, and then the eventual recovery of the circuit as the capacitor again charges to the full impressed potential.

In either case, the radiation-induced conductance is defined in terms of the observed voltage signal by the following analysis.

$$-\frac{V}{R} = G(E_0 + V) + C \frac{d(E_0 + V)}{dt}, \quad (1)$$

Table 1
CAPACITOR TYPES SELECTED FOR TESTING ON GGA LINAC

Dielectric Type	Manufacturer	ϵ (Dielectric Constant)	$C_{nom.}$ (μF)	$C_{meas.}$ (μF)	W.V. (Volts)
Al_2O_3	Sprague	7.0	1.0	0.86	150
Al_2O_3	Sprague	7.0	1.0	0.88	150
Al_2O_3	Sprague	7.0	10	11.4	50
Ceramic	Hi-Q	500.0	0.01	---	50
Ceramic	Hi-Q	500.0	0.01	---	150
Ceramic	CRL		0.1	0.1	75
Glass	Corning	8.4	0.01	0.0099	600
Glass	Corning	8.4	0.01	0.0102	600
Teflon	Component Research	2.0	0.01	0.0100	50
Teflon	Component Research	2.0	0.01	0.101	50
Teflon	Component Research	2.0	1.0	1.01	50
Polystyrene	Mallory	2.5	0.01	0.01	600
Polystyrene	Mallory	2.5	0.01	0.0102	600
H-Film	TRW	3.1	0.3	0.332	50
H-Film	TRW	3.1	0.3	0.314	50
H-Film	TRW	3.1	0.06	0.066	200
H-Film	TRW	3.1	0.06	0.063	200
Vitamin Q	Sprague	3.0	0.01	0.0094	100
Vitamin Q	Sprague	3.0	0.01	0.0094	100
Vitamin Q	Sprague	3.0	0.1	0.098	100
Polycarbonate	Aerovox	3.0	0.1	0.925	100
Polycarbonate	Aerovox	3.0	0.1	---	100
Tantalum Oxide (foil)	Sprague	24.0	3.0	3.0	75
Tantalum Oxide (foil)	Sprague	24.0	3.0	3.20	75
Mylar	Elpac	3.0	1.0	0.095	100
Mylar	Elpac	3.0	1.0	1.14	100
Mica	Cornell Dublier	7.0	0.001	0.00098	600

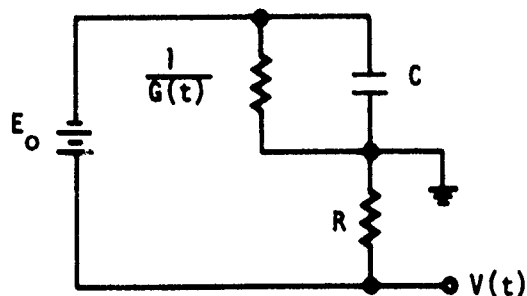


Fig. 1. Test circuit schematic

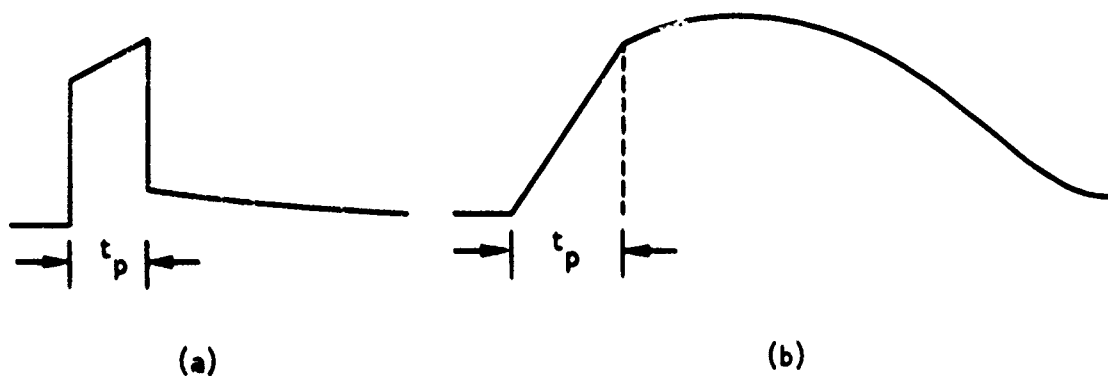


Fig. 2. Current signals induced by radiation pulse

$$G = - \frac{V}{R(E_0 + V)} - \frac{C}{E_0 + V} \frac{d(E_0 + V)}{dt} . \quad (2)$$

The difficulty with this formulation is that the derivative in the last term is a particularly poor mathematical term to calculate accurately by computer techniques from empirical data at late times. It involves obtaining small differences between large numbers, and thus, small fluctuations can cause large errors.

This difficulty has been overcome in the past⁽³⁾ by calculating the integral of the conductance, i.e.,

$$\int_0^t G dt = -\frac{1}{R} \int_0^t \frac{V dt}{E_0 + V} - C \int_0^t \frac{d(E_0 + V)}{(E_0 + V)}, \quad (3)$$

$$\int_0^t G dt = -\frac{1}{R} \int_0^t \frac{V}{E_0 + V} dt - C \ln(E_0 + V). \quad (4)$$

The conductance integral data were then differentiated graphically to obtain the desired conductance. This technique works and has been successfully used in the past. However, to process the amount of data necessary to obtain dose and dose rate information for all the dielectrics being considered in this study, a more rapid and less arduous method than graphical differentiation was employed.

Once the conductance data were obtained, it was desired to analyze it in the formulation of Ref. 2 to obtain the fitting parameters of that formulation. The radiation-induced conductivity as described in this reference is

$$\sigma = \sigma_p + \sum_i \sigma_{di}, \quad (5)$$

where, for short-pulsed radiation with 30-MeV electrons,

$$\sigma_p = F_p(\gamma) \dot{\gamma}, \quad (6)$$

$$\sigma_{di} = F_{di}(\alpha) \int_{-\infty}^t \dot{\gamma}(t') \exp[-(t - t')/\tau_{di}] dt', \quad (7)$$

where

$$\alpha = \gamma, \quad t_p < \tau_{di}; \quad \alpha = \dot{\gamma}\tau_{di}, \quad t_p > \tau_{di} . \quad (8)$$

In these equations:

- σ = radiation-induced total conductivity,
- σ_p = prompt portion of the conductivity,
- σ_{di} = i^{th} delayed conductivity component,
- $F_p(\gamma)$ = prompt conductivity fitting parameter which may be a function of total dose,
- $\dot{\gamma}$ = instantaneous dose rate during the pulse,
- $F_{di}(\alpha)$ = fitting parameter of the i^{th} delayed component and is a function of the dose rate times the pulse width ($\dot{\gamma}t_p = \gamma$) if the pulse width is shorter than the i^{th} decay constant or the dose rate times the decay time for pulse widths longer than the decay constant,
- τ_{di} = decay constant of the i^{th} delayed component, which may vary during the decay.

Since

$$G = \frac{C}{\epsilon\epsilon_0} \sigma , \quad (9)$$

where ϵ is the dielectric constant, and

$$\dot{\gamma} = \beta, \quad 0 < t < t_p, \quad \dot{\gamma} = 0, \quad t_p < t < \infty \quad (10)$$

and letting

$$A = \frac{C}{\epsilon\epsilon_0} , \quad (11)$$

Eq. 5 may be written

$$G = A F_p \dot{Y} + \sum_i A F_{di} \int_{-\infty}^t \dot{Y} \exp[-(t - t')/\tau_{di}] dt' . \quad (12)$$

In the course of the analyses, we found that τ_{di} both varied with time following the pulse and was a function of the dose. Hence, a presentation of the data was developed which did not involve fitting the data to an exponential function over the entire length of the decay.

A very useful quantity for circuit response prediction is the charge flow per unit dose per unit capacitance per unit applied voltage, which we will call the specific charge release. For the prompt component, the specific charge release is represented by

$$Q_p = F_p / \epsilon \epsilon_0 = \frac{1}{\gamma C} \int_0^{t_p} G dt , \quad (13)$$

where t_p is the pulse width for short pulses. This quantity is used to represent the prompt conductivity.

For the delayed components, the specific charge release is computed for intervals of time after the pulse.

$$\Delta Q_{12} = \frac{1}{\gamma C} \left[\int_{t_1}^{t_2} G dt \right] \quad (14)$$

for the time interval from t_1 to t_2 . To allow easy interpolation, the points in each interval are fitted to a single exponential.

$$\begin{aligned}
\Delta Q_{1t} &= \frac{1}{\gamma C} G_o \int_{t_1}^t e^{-t/\tau_{12}} dt \quad t \leq t_2 \\
&= \frac{1}{\gamma C} G_o \tau (e^{-t_1/\tau_{12}} - e^{-t/\tau_{12}}) \\
Q_o &= \frac{1}{\gamma C} G_o \quad .
\end{aligned} \tag{15}$$

The total specific charge release at any time t after pulse is obtained by simply summing the amount of specific charge release in each interval, i.e.,

$$Q_t = Q_p + \sum_{i=1}^n \Delta Q_{1,i+1} + \Delta Q_{n+1,t} \quad , \tag{16}$$

where n is the number of complete intervals prior to the time t . If the τ 's derived above are constant for adjacent intervals, then the decay can be represented by a single exponential over these intervals.

In order to verify the linear dependence of the induced conductivity on the dose rate for constant dose and to measure the dose dependence for constant dose rate, the irradiation program shown schematically in Fig. 3 was followed as closely as possible for each capacitor. The diagonal lines represent the dose-versus-dose-rate relationships for the pulse widths nominally available with the GGA Linac. The grid of points on these lines shows the exposures given the capacitors. Sometimes experimental conditions precluded obtaining data at some of the highest and lowest dose points, but in general, the plan shown in Fig. 3 was followed.

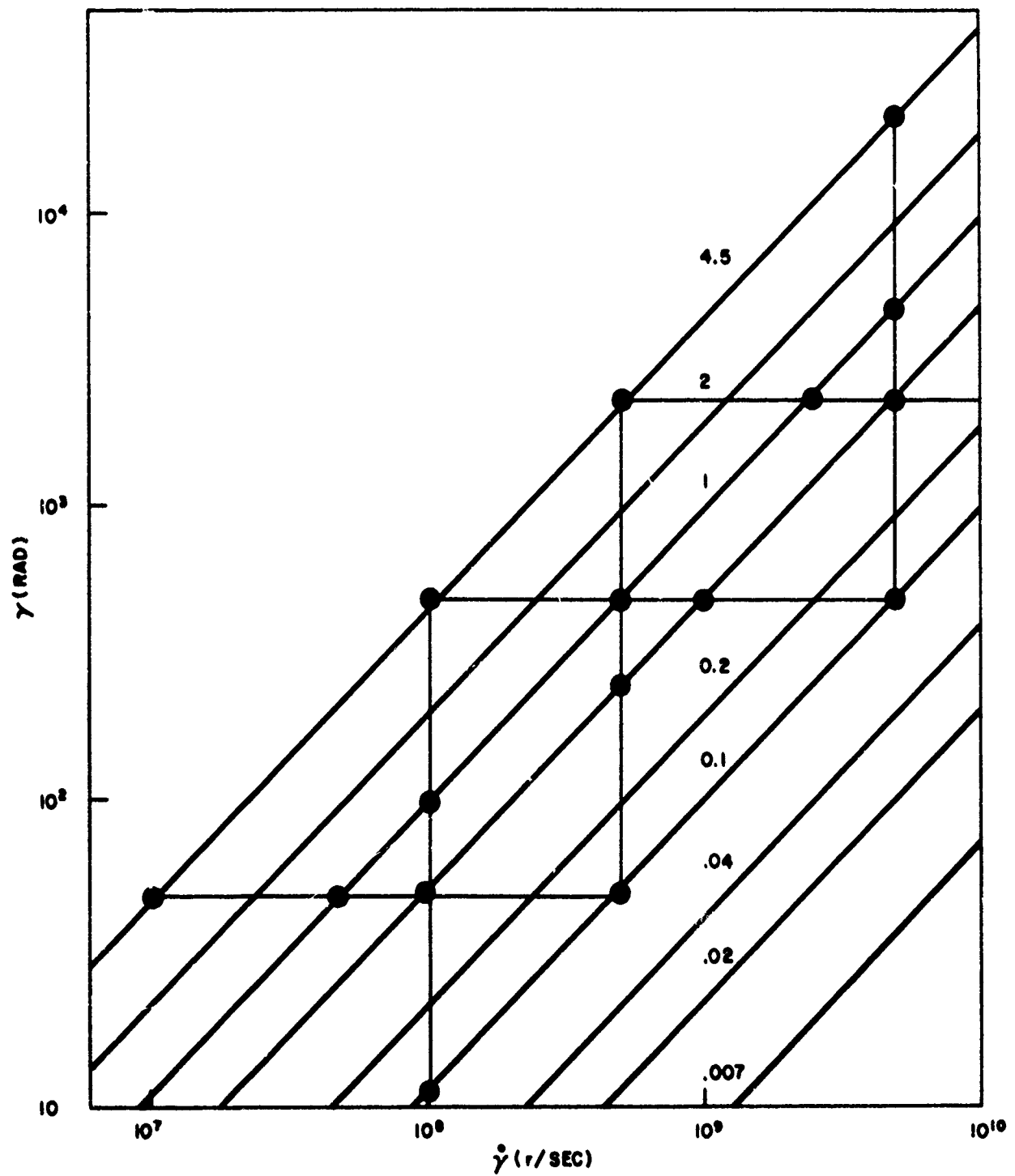


Fig. 3. Diagram showing the data points taken during L'nae experiments with pulse widths in μsec

3. RESULTS AND DISCUSSION

The results are presented in Tables H-1 through H-11 in Appendix A. The data are tabulated by dielectric type. Beside the name of each material type is listed the number of capacitors of each capacitance value tested and the working voltage of each. As there were no capacitance-value-correlated trends in the data, the listings include data from all units, and the values given are usually averages over many test exposures.

The dose is listed in rads (Si) for convenience. Since for high-energy electron energy deposition the energy deposited scales very nearly as Z/A , the doses can be considered as rads (dielectric material).

The radiation pulse width and the decay constants (τ) are given in microseconds.

The Q_p and ΔQ values are in units of coulombs per farad-volt-rad, and the Q_0 values are in units of coulombs per farad-volt-rad- μ sec.

Where a definite voltage dependence of the specific charge release was observed, it is noted at the bottom of the listing.

Lack of Q_0 and τ data for time intervals in which a ΔQ is listed implies that a linear interpolation may be used for obtaining intermediate points.

In general, the function F_p appears to vary only slightly with dose, if at all. Slight decreases in the prompt specific charge release are observed in some materials as the dose is increased, but this may be due to a buildup of internal polarization during the larger-dose pulses. A deviation from a linear dependence on dose rate would appear in differences in values of Q_p for the same dose but with different pulse widths. Within the experimental scatter in the data, this is not observed. Hence, the model is verified to within the precision of the experiment.

The scatter observed in the data is somewhat larger than expected, and there are a number of possible reasons for this. Differences between two capacitors, apparently inherent in off-the-shelf units, account for a portion of the scatter. Units of the same type and having the same electrical characteristics can differ considerably in their radiation response. Another source of experimental error can arise if the capacitor is not completely depolarized between test exposures. Although attempts were made to depolarize the capacitors by exposing the shorted capacitors to ten or more Linac pulses between test exposures, small remnant polarization fields may have contributed to the scatter.

The delayed components posed a particularly difficult problem in our attempts to match theory with experiment. The data reduction scheme employed involved the fitting of the decay of the delayed conductivity to the sum of two exponentials. This was accomplished by arbitrarily selecting initial values for the time constants and then varying them until a least square error function, computed using the data points, was minimized. This routine fit some artificial trial data sets quite well. When the capacitor data were processed using this fitting routine, exponentials were determined which fit a particular exposure, but no consistency could be obtained between exposures. Upon examination, we found that a two-exponential, four-parameter fit to the decays was too sensitive to slight scatter in the experimental points. In addition, we found many of the decays appeared more hyperbolic than exponential, and that the decay times were a function of the dose. Thus, the delayed charge release in certain time intervals after the pulse is presented, since relatively consistent results came from this scheme. It is possible that a detailed examination of the decays may reveal that exponential decay laws are followed, but this is not apparent from the computer data analysis, and too many records are involved to carry out such an examination under this contract.

H. CAPACITORS

INTRODUCTION

Most of the electronic properties of capacitors are affected by nuclear radiation to some extent. Changes in the capacitance value, dissipation factor, and leakage resistance have been observed during steady-state reactor experiments. These effects are generally not considered severe for fast neutron fluences less than 10^{15} n/cm² ($E > 10$ keV, fission), and for most capacitors this limit is about 10^{17} n/cm² ($E > 10$ keV, fission). (1)

Effects of pulsed radiation on the capacitance value have been shown to be less than 0.1 percent for frequencies of the applied signal up to about 200 kHz. Dissipation-factor measurements made before and after irradiation indicate no clear trend in the effect on this parameter, although changes in the range of ± 20 percent have been observed. However, during a high-intensity pulse of nuclear radiation, the most pronounced effect in a capacitor is a transient change in the conductivity of the dielectric material with a corresponding increase of the leakage currents through the capacitor. The properties of these transient changes in conductivity are the subject of this section.

During the past several years, the concept of ionization effects in insulating and dielectric materials has undergone a critical review and redevelopment.* As a result of this work, the Nichols-van Lint Track Model, a more accurate description of the phenomena involved, has been developed. (2, 3) Based on this model, a prediction of the changes in conductivity of a capacitor dielectric (and, of course, directly relatable parameters, e.g., capacitor voltage and current) due to transient ionizing radiation can be made. (4) The Nichols-van Lint Track Model deviates from past descriptions in that ionizing particles are described as creating ionized tracks in the irradiated material. For normal TREE simulation, this means that, microscopically, the material is not uniformly ionized. (An exception to this occurs at very high dose rates, $\sim 10^{12}$ rads/sec, where there should be sufficient overlap of the ionized tracks for the material to be considered uniformly ionized.)

*This section is developed primarily for the design engineer and, as such, does not involve details of the physics of the theory presented. Those persons interested in that type of discussion can find detailed development of the theory in Refs. 2, 3, and 4. Only a general outline of the main points of theory is included here.

RADIATION-INDUCED CONDUCTIVITY

The excess conductivity induced in a material irradiated with a short pulse of ionizing radiation is generally discussed in terms of two general classifications-- the prompt component and the delayed component. The prompt component is primarily the result of excess carrier concentration from direct ionization by the radiation and the concurrent recombination and trapping of these carriers. The delayed component is considered as that component of conductivity remaining after the termination of the ionizing pulse, and is the result of thermal generation of excess carriers from shallow traps, in which they are caught during the prompt pulse, and their concurrent loss to recombination and retrapping. The rate at which these carriers are thermally regenerated is dependent on the energy level of the trap site, the concentration of filled traps, and the temperature. As there is usually more than one energy level trap in a material, more than one regeneration rate is usually observed in the delayed component.

The excess conductivity is proportional to the number of carriers available to drift under the influence of the applied electric field. However, the microscopic nonuniformity of the carrier concentration must be considered for the pulsed irradiation case. For irradiation with ionizing particles with a low specific ionization (the ratio of the number of ion pairs produced per unit path length to the number produced per unit path length by a minimum ionizing particle), the excess prompt conductivity will be the same as if these carriers were generated uniformly throughout the material. However, if the specific ionization is increased (by bombardment with more heavily ionizing particles), a point will be approached where the separation of ionization sites is less than the distance traveled by the electron before it has become thermalized and is able to drift under the influence of the applied electric field. As this point is approached, the probability that the electron will be captured in the Coulomb field of a neighboring ion increases, and the contribution to excess conductivity will be reduced. Thus, a plot of prompt conductivity (σ_p) versus specific ionization (S) would show σ_p constant at low S and slowly decreasing after some threshold S value is reached.

The rate at which carriers are lost concurrent with their generation by the ionizing radiation is proportional to the concentration of recombination centers and unfilled trapping centers. On this point, a big difference is clearly evident between the old formulation for ionization induced conductivity and the track model. While an insignificant number of the total traps in the material might be filled at low doses, the concentration of filled traps within a track depends only on the specific ionization. Thus, the trapping rate is affected by the specific ionization. The result of this effect is to cause an increase in prompt conductivity with specific ionization, which would serve in part to compensate for the decreasing effect mentioned above. However, this effect on the carrier loss rate should be slight, as most of the carriers are lost to recombination rather than trapping. It was consideration of the effects of trap-filling during prolonged irradiations which led to the prediction⁽⁵⁾ of nonlinear dose-rate dependences in the formulation of radiation-induced conductivity used in earlier TREE Handbook Section H editions.

When the radiation is delivered in a time short compared with the regeneration time of carriers from the traps, and the dose delivered in the pulse is large enough that significant numbers of tracks near the end of the pulse overlap tracks generated earlier, then the concentration of filled traps in a track late in the pulse is different from that in a track through previously unirradiated material. When this occurs, the observed prompt conductivity becomes a function of the total dose delivered in the pulse, as well as of the specific ionization of the irradiating particle.

The delayed conductivity component depends on the rates of carrier regeneration and retrapping from trap sites which, in turn, are dependent on the concentration of filled traps and the energy levels of the traps. The concentration of filled traps is a function of the specific ionization of the irradiating particle and, in the case of overlapping tracks, the total dose. As the initial concentration of filled traps within a track is usually a significant fraction of the total concentration of traps, the retrapping probability changes during the time the traps are emptying, thus altering the characteristic time for emptying the remainder of the filled traps. As a result, the decay of the delayed component does not usually follow a simple law. Only in certain cases, where the trapping probability is negligibly perturbed by the radiation, will simple exponential decays be observed. Thus, in the presentation of the data, no attempt has been made to fit the entire decay to exponential laws, but it will be apparent from the presentation when an exponential law is followed for a portion of the decay.

NEUTRON-INDUCED CONDUCTIVITY

Neutrons produce ionization by a number of collision processes that give rise to ionizing secondary particles. These processes include:

1. Elastic scattering when the recoil atom receives sufficient energy to produce ionization,
2. Inelastic scattering, producing a recoil atom that may or may not ionize but that emits a gamma photon that can produce a secondary ionization,
3. Capture, resulting in the emission of a photon and/or an ionizing secondary particle (primarily thermal neutrons),
4. Reactions resulting in an ionizing particle, e. g., (n, p) or (n, α) reactions (high-energy neutrons).

There are, therefore, many possible different specific ionizations associated with ionized tracks in neutron-bombarded materials.

In hydrogenous materials, the principal ionization is caused by recoil protons which have a high specific ionization. For this reason, neutron-induced conductivity in hydrogenous dielectrics has been found to be approximately one-fifth to one-half

that of gamma-ray-induced conductivity for equal ionization-energy deposition rate. For nonhydrogenous dielectrics, the most important contribution to neutron-induced ionization is by the interactions of very high-energy neutrons ($E > 2$ MeV).

One method which has been used for obtaining a rough estimate of neutron-induced conductivity was to compare currents induced in capacitors by a pulsed nuclear reactor with those induced by a high-intensity electron beam pulse (18 MeV).⁽⁶⁾ Prompt and delayed conductivity coefficients were calculated from these data, and it was concluded on the basis of these results that the ratios of the prompt and delayed components for neutrons are equal to those for the electrons. This, of course, indicates that the specific ionization of the secondary particles in the neutron irradiation was not high enough to appreciably change the occupation of the trapping sites.

When estimating ionization effects due to neutrons, the neutron pulse is used in the calculations. For calculations based on a weapon environment where radiation-induced conductivity due to both the neutrons and the gamma rays is being combined, the difference in the arrival time of the two radiation pulses must be considered.

POLARIZATION EFFECT

A "polarization effect" that is attributed to space charge buildup within the dielectric material due to nonuniform trapping has been observed with some capacitors, particularly with Mylar, mica, polycarbonate, and tantalum oxide devices.⁽⁷⁾ This effect is manifested in several ways. One of these is an apparent decrease in the induced conductivity with sequential radiation pulsing. Charge transfer across the dielectric during a radiation pulse builds up a space charge field opposing the applied electric field. If the applied electric field is then removed, subsequent radiation pulses result in a current in the external circuit opposite in direction to that observed with the field applied. This is caused by the discharge of the space charge field. Similarly, if the electric field is reversed rather than removed after the space charge has been built up, the space charge field enhances the applied field, and a larger current results than would be observed normally.

Saturation of the polarization effect, where no further decrease in the charge transfer is observed with subsequent radiation pulses, occurs after one or more pulses, depending on the capacitor and on the dose delivered in each pulse. Decreases of 50 to 70 percent for mica, 10 to 20 percent for tantalum oxide, and 30 percent for Mylar have been observed due to this space charge buildup during radiation pulsing.⁽⁵⁾

A model which accounts for these effects has been proposed, but at this time is not amenable to device prediction.⁽⁶⁾

ENGINEERING DATA

All data given in this section are for room-temperature irradiation. Although there is evidence that the conductivity effect should depend on temperature, and this

is to be expected theoretically, insufficient data are available on this dependence to be included here. Some data on the response of tantalum and ceramic capacitors as a function of temperature can be found in Ref. 8.

Variations in materials or construction are probably largely responsible for the scatter in results obtained from irradiation of commercially available capacitors. In some cases, capacitors whose electrical characteristics are very nearly equal will respond differently to a radiation burst. Differences as large as a factor of five have been observed. Further uncertainty in capacitor data in the literature arises inherently from the techniques used by different experimenters in the measurement of the conductivity, the exposure rate, and the total exposure during the radiation pulse.

All of the data in this section were taken at one facility using one measurement technique and one dosimetry technique, but there is still considerable scatter.

Experimental Techniques and Data Handling

The experiments reported here were conducted using a battery-pack power supply from which voltages of 300, 180, 90, 45, 22.5, and 12 volts were available. The highest of these voltages which did not exceed the rated working voltage of the capacitor was usually used, as were the next two lower voltages. In many capacitor types, a voltage dependence of the specific charge release, Q_p was noted during these tests. Q_p was higher for the lower applied voltages by 10 to 50 percent although exceptions were occasionally noted where the lower voltage Q_p s were higher by a factor of 2 to 5.

This voltage dependence is believed to be the result of a voltage-dependent barrier at the contacts between the dielectric materials and their metal electrodes. This belief is substantiated by the fact that values of charge transfer that would be calculated from previous conductivity data on some of the dielectric materials tested are higher by as much as a factor of 10 than those measured in these capacitor tests. Much of the data on dielectric material radiation-induced conductivity was collected on laboratory samples in which great care was taken to get the best contact possible between the dielectric and the electrode. This results in higher apparent induced-conductivity in such samples compared to the capacitor tests.

The capacitors were irradiated in the circuit shown schematically in Fig. H-1. The radiation source was a 30-MeV electron beam from a linear accelerator, and pulse widths ranging from 0.1 to 4.5 μ sec were used. The capacitors were mounted on a wheel in an evacuated chamber and rotated into position in the beam for testing. The voltage, V , developed across the series measuring resistor, R , was the parameter monitored.

For each irradiation pulse, the voltage transient was sampled at 30 points in time and the 30 voltage levels recorded on magnetic tape along with subsidiary data, e.g., amplifier gains, applied voltage, sampling span, etc. The tape data were then fed directly to a UNIVAC 1108 computer for analysis.

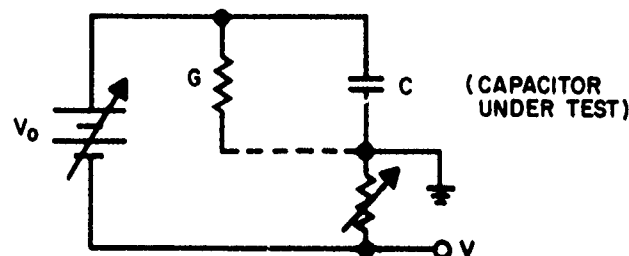


Fig. H-1. Schematic of capacitor test circuit

The analysis of the data was performed in the following manner, based on the circuit of Fig. 1.

$$-\frac{V}{R} = G(V_O + V) + C \frac{d}{dt} (V_O + V), \quad (1)$$

$$G = -\frac{1}{R} \left(\frac{V}{V_O + V} \right) - \frac{C}{V_O + V} \frac{d}{dt} (V_O + V), \quad (2)$$

$$\int_0^t G dt = -\frac{1}{R} \int_0^t \frac{V}{V_O + V} dt - C \int_0^t \frac{1}{V_O + V} \frac{d}{dt} (V_O + V) dt, \quad (3)$$

$$\int_0^t G dt = -\frac{1}{R} \int_0^t \frac{V}{V_O + V} dt - C \int_{V_O}^{V_O + V} \frac{d\theta}{\theta}, \quad (4)$$

$$\int_0^t G dt = -\frac{1}{R} \int_0^t \frac{V}{V_O + V} dt - C \ln \frac{V_O + V}{V_O}, \quad (5)$$

where V_O is the applied voltage,

R is the current monitoring resistor,

C is the capacitor under test,

G is the radiation-induced conductance of the capacitor dielectric,

V is the voltage developed across R , and

$V_O + V$ is the voltage across the capacitor.

The integral of the conductance was calculated to avoid the use of differentials which are prone to large errors in this type of machine calculation. The shape of a typical integrated conductance versus time plot is shown in Fig. H-2.

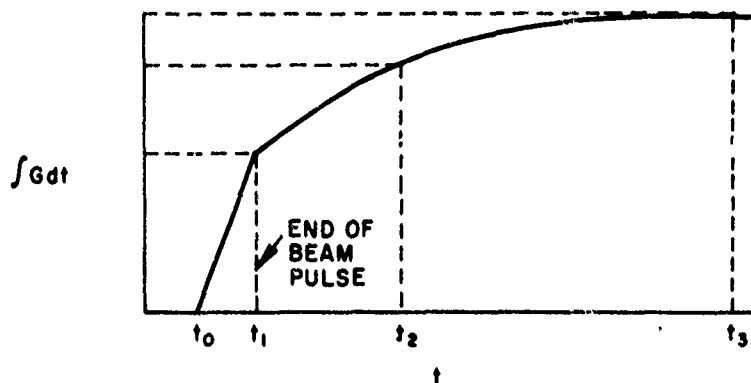


Fig. H-2. Integral of conductance versus time

From such data, the specific charge release was calculated. The results are tabulated in the next section in the following manner.

$$Q_p = \frac{1}{\gamma C} \int_0^{t_1} G dt \quad (6)$$

$$\Delta Q_{a-b} = \frac{1}{\gamma C} \int_{t_a}^{t_b} G dt \quad (7)$$

where Q_p represents the prompt charge transfer per applied volt per farad per rad absorbed during the pulse, and ΔQ_{a-b} represents the additional specific charge release during the period t_a to t_b .

In addition, for those time intervals in which the specific charge release could not be considered linear with time, two additional parameters are listed: Q_0 and τ . With the use of these two parameters, the additional specific charge release to any time within a specified time interval can be calculated as

$$\Delta Q_{a-x} = Q_0 \tau \left(1 - e^{-\frac{(t_x - t_a)}{\tau}} \right). \quad (8)$$

EXAMPLE. The charge release to 500 μ sec after a 680-rad gamma pulse is required for a .01 μ F polystyrene capacitor initially charged to 50 volts.

From the table,

$$\begin{aligned} Q_p &= 2.0 \times 10^{-6}, \\ \Delta Q_{10} &= 2.8 \times 10^{-7}, \\ \Delta Q_{10-30} &= 3.3 \times 10^{-7}, \\ \Delta Q_{30-100} &= 2.2 \times 10^{-6}, \\ \Delta Q_{100-300} &= 2.4 \times 10^{-6}. \end{aligned}$$

For the interval from 300 to 500 μ sec,

$$\Delta Q_{300-500} = 1.0 \times 10^{-8} \times 5 \times 10^2 \left(1 - e^{-\frac{200}{500}} \right) \approx 1.7 \times 10^{-6}.$$

The total specific charge release is the sum of all these contributions, i. e. ,

$$Q_{\tau} = 8.9 \times 10^{-6} \text{ coul/rad/Farad/Volt,}$$

and the total charge transfer to 500 μ sec is

$$8.9 \times 10^{-6} \frac{\text{coul}}{\text{rad-farad-volt}} \times 10^{-8} \text{ farad} \times 680 \text{ rad} \times 50 \text{ volt} = 3.0 \times 10^{-9} \text{ coul.}$$

The voltage drop in the absence of charging during this time would be

$$\Delta V = \frac{\Delta Q}{C} = \frac{-3.0 \times 10^{-9}}{10^{-8}} = -0.3 \text{ volt.}$$

TABULATIONS

The data are tabulated by dielectric type. Beside the name of each material type is listed the number of capacitors of each capacitance value tested and the working voltage of each. As there were no capacitance-value-correlated trends in the data, the listings include data from all units.

The dose is listed in rads (Si) for convenience. Since for high-energy electron energy deposition, the energy deposited scales very nearly as Z/A , the doses can be considered as rads (dielectric material).

The radiation pulse width and the decay constants (τ 's) are given in microseconds.

The Q_p and ΔQ values are in units of coulombs per farad-volt-rad, and the Q_0 values are in units of coulombs per farad-volt-rad- μ sec.

Where a definite voltage dependence of the specific charge release was observed, it is noted at the bottom of the listing.

Lack of Q_0 and τ data for time intervals in which a ΔQ is listed implies that a linear interpolation may be used for obtaining intermediate points.

While longer time constant decays certainly exist, no charge release past 3000 μ sec was measured during these tests.

Table H-1

TANTALUM OXIDE (2 - 3 μ F, W.V. 75) (foil)

Dose [rads(Si)]	Pulse Width (μ sec)	Q_p	ΔQ_{30}	ΔQ_{300}
70	0.5	1.0-06		
110	0.9	1.4-06		1.6-06
234	0.2	1.6-06		2.6-06
360	3.9	1.0-06		1.7-06
450	0.9	1.4-06		
1,250	0.5	1.0-06		
1,700	3.9	6.0-07		
2,200	0.9	8.0-07	1.3-06	
11,000	3.9	6.0-07		6.6-07

NOTE: Extremely erratic results for this type have resulted in minimal meaningful interpretation for these data.

Table H-2

POLYCARBONATE (3 - 0.1 μ F, W.V. 100) (Prompt Responder)

Dose [rads(Si)]	Pulse Width (μ sec)	Q_p (coul/farad-volt-rad)
10	0.1	1.5-05
16	0.16	1.0-06
45	0.5	2.0-06
56	0.1	2.6-06
70	1.3	1.8-06
80	0.16	1.5-06
100	0.9	1.7-06
190	0.2	5.2-06
250	0.1	2.4-06
360	3.9	1.8-06
450	0.9	1.2-06
500	0.5	1.0-06
680	0.2	1.5-06
1,250	0.5	1.7-06
1,700	3.9	1.3-06
2,200	0.9	1.4-06
5,500	1.0	1.5-06
11,000	3.9	1.4-06

NOTE: Values are for 45V applied. For 90V or 22.5V applied, the values of Q_p decrease and increase by about 30% respectively.

Table H-3

ALUMINUM OXIDE (2 - .01 μ F, W.V. 150; 1 - 10 μ F, W.V. 50) (Prompt Responder)

Dose [rads(Si)]	Pulse Width (μ sec)	Q_p (coul/farad-volt-rad)
34	0.8	2.0-06
40	2.7	1.5-06
68	0.8	1.2-06
70	1.3	2.2-06
100	0.9	2.9-06
360	3.9	4.0-06
420	0.8	1.9-06
450	0.9	1.8-06
1250	0.5	2.0-06
2200	0.9	1.7-07
2200	1.0	8.0-07
5500	1.0	5.0-07

NOTE: Some delayed components were observed at exposures of 680 rads (0.2 μ sec).
 The total delayed charge release during these exposures was about 10^{-6} coul/farad-volt-rad.

Table H-4
POLYSTYRENE (2 - .01 μ F, W.V. 600; 1 - .001 μ F, W.V. 600)

Dose [rads(Si)]	Pulse Width (μ sec)	Q_p	ΔQ_{10}	ΔQ_{10-30}^*	30-100 μ sec		100-300 μ sec		300-1000 μ sec		
					ΔQ	Q_0	ΔQ	Q_0	ΔQ	Q_0	τ
10	0.1	2.6-06	3.2-07	3.3-07	2.6-06		5.7-06	3.6-08	3.0-06		300
34	0.8	1.9-06		2.1-07	1.1-06		2.0-06	1.7-08		9.0-09	500
37	2.7	3.3-06		1.3-06	2.3-06	4.0-08	2.9-06	2.5-08			220
56	0.1	3.0-06	3.9-07	9.6-07	3.6-06		8.4-06	5.0-08			600
68	0.8	1.3-06	2.2-07	4.4-07	1.4-06	2.0-08	2.1-06	1.4-08	3.2-06	6.0-09	1000
70	1.3	4.0-06									
80	0.16	1.2-06									
110	0.8	5.0-06									
234	0.5	5.0-06									
250	0.1	3.3-06	6.7-07	1.3-06	5.6-06	6.0-08	1.1-05				
345	2.3	2.2-06	5.3-07	9.5-07	2.0-06	5.2-08	2.2-06	2.0-08			170
360	3.9	3.4-06									
450	0.8	5.5-06									
500	0.5	5.0-06									
500	0.8	2.5-06	5.0-08	3.5-08	3.5-07		3.7-07				
680	0.2	2.0-06	2.8-07	3.3-07	2.2-06	3.9-08	2.4-06	2.1-08	3.2-06	1.0-08	500
1,250	0.5	5.5-06									
5,500	1.0	2.9-06		7.5-07	1.7-06	3.7-08	1.7-06	1.7-08			
11,000	3.9	6.5-06	9.6-07	1.2-07	1.4-06	3.5-08					
12,000	3.5	2.3-06									

* Where no entry for ΔQ_{10} is given, ΔQ_{10-30} is the specific charge release from the end of the beam pulse to 30 μ sec.

Table H-5

NOTE: Values are for 22V applied. Add -30% and +30% for 45V and 22V respectively.

Table H-6
H-FILM (2 - .06 μ F, W.V. 200)

Dose [rads(Si)]	Pulse Width (μ sec)	Q_p^*	ΔQ_{30}^*	30-100 μ sec		100-300 μ sec	
				ΔQ^*	Q_0	ΔQ^*	Q_0
4.1	0.1	1.5-06	4.8-07	7.0-07	1.4-08	7.7-07	8.1-09
20	0.1	1.1-06	3.7-07	5.0-07	9.0-09	6.1-07	5.0-09
40	3.0	2.2-06	7.3-07	9.8-07	2.2-08	1.1-06	8.1-09
45	0.65	1.8-06	5.8-07	6.3-07	1.5-08	5.3-07	4.0-09
200	0.1	1.3-06	4.2-07	5.0-07	1.2-08	5.2-07	4.0-09
260	0.65	1.7-06	5.5-07	6.0-07	1.5-08	6.0-07	5.0-09
360	3.0	2.3-06	7.4-07	7.7-07	2.0-08	8.6-07	7.5-09
520	0.65	1.6-06	5.0-07	5.6-07	1.3-08	5.0-07	4.1-09
1,300	3.1	1.7-06	6.0-07	6.0-07	1.6-08	6.0-07	5.0-09
2,000	0.65	2.0-06	6.0-07	7.2-07	1.7-08	6.8-07	5.1-09
11,000	4.0	1.6-06	5.0-07	5.0-07	1.3-08	5.8-07	4.1-09
							115
							230
							230
							230
							185
							185
							155
							170
							150
							160
							135

NOTE: Values are for 90V applied. Add +15% and -15% for 45V and 180V, respectively, for the Q_p .
For the ΔQ , add +15% and -15% for 180V and 45V, respectively.

Table H-7

Dose [rads(Si)]	Pulse Width (μ sec)	Q_p	ΔQ_{10}	ΔQ_{10-30}	30-100 Q_0		100-300 Q_0		300-1000 Q_0		τ
					ΔQ	τ	ΔQ	τ	ΔQ	τ	
40	2.7	9.0-07									
56	0.1	1.4-06	1.2-06	7.6-07	4.7-06		1.1-05				
250	0.1	1.6-06	1.0-06	1.6-06	9.7-06		2.3-05				
350	2.3	7.8-07		1.6-06*	2.9-06	170	3.6-06	170			
600	0.8	1.0-06	9.0-08	4.0-07	5.0-07		2.5-06				
680	0.2	1.6-06									
5,500	1.0	4.7-07					1.6-06*				
11,000	3.5	8.4-07	1.7-07	1.5-06	9.0-07	30	5.6-07	170	3.8-06	1.6-08	450

* Total delayed charge release since end of beam pulse.

Table H-8
MYLAR (2 - 1 μ F, W.V. 100)

Dose [rads(Si)]	Pulse Width (μ sec)	Q_p	ΔQ_{30}	ΔQ 30-100 μ sec Q_0	τ	ΔQ 100-300 μ sec Q_0	τ	ΔQ 300-1000 μ sec Q_0	τ
45	0.2	3.5-06							
70	0.5	1.9-06							
110	0.9	2.0-06							
234	0.2	2.5-06	6.8-07	5.5-07		5.6-07		3.6-07	
360	3.9	3.2-06	3.0-07			1.0-06		8.0-07	
450	0.9	2.6-06	9.0-07			9.0-07	100	8.0-08	95
500	0.5	2.0-06							
1,250	0.5	1.6-06	1.0-06						
1,700	3.9	1.3-06		1.9-07		1.5-07		2.8-07	
2,200	0.9	1.1-06	4.2-07	5.4-07		3.7-07		6.2-07	
11,000	3.9	1.4-06							

NOTE: Values given are for 45V. Add -30% or +30% for 90V and 22V, respectively.

Table H-9
VITAMIN Q (2 - .01 μ F, W.V. 100; 1 - 0.1 μ F, W.V. 100)

Dose [rads(Si)]	Pulse Width (μ sec)	Q_p	30-100		100-300		300-1000		1000-3000	
			ΔQ_{30}	Q_o	ΔQ	Q_o	ΔQ	Q_o	ΔQ	Q_o
10	0.1	1.4-05	5.3-06	1.2-05	2.4-05					
16	0.2	3.5-06								
34	0.8	1.1-05								
45	0.5	1.8-06								
44	2.7	1.3-05	4.0-06	2.0-06	5.0-06	5.0-08	130			
56	0.1	1.0-05								
68	0.8	1.4-05	3.6-06	4.8-06	2.3-06	3.0-08	100			
70	1.3	1.6-06	6.0-07	2.4-07	2.3-07			1.6-06	3.4-07	1000
81	0.2	2.0-06								
110	0.9	1.6-06	9.0-07	5.0-07	1.8-06			2.8-06	4.0-09	600
190	0.2	9.1-06								
234	0.5	2.5-06								
250	0.1	1.4-05	3.4-06	6.5-06						
360	3.9	2.1-06								
450	0.8	1.3-06	4.4-07	1.0-06		1.8-08	380			
500	0.5	2.1-06								
680	0.2	5.5-06	4.5-06	2.4-06	3.1-06	3.1-08	140			
1,250	0.5	2.0-06								
1,400	2.4	3.1-06	5.1-07	1.2-06						
2,200	0.9	1.9-06								
2,500	0.1	1.2-06								
5,500	1.0	3.3-06	8.6-07	2.2-06	2.9-06	2.4-08	150			
11,000	3.9	1.8-06	2.9-07	8.3-07	2.0-06	1.3-08	320	4.4-06	7.7-09	1900

NOTE: (1) Values of Q_p are for 45V applied. Add -30% or +30% for 90V and 22 volts, respectively.
(2) Large scatter in data probably due to the fact that Vitamin Q capacitors polarize strongly.

Table H-10
GLASS (2 - .01 μ F, W.V. 600; 1 - .001 μ F, W.V. 600)

Dose [rads(Si)]	Pulse Width (μ sec)	Q_p	30-100		100-300		300-1000		1000-3000			
			ΔQ	Q_o	τ	ΔQ	Q_o	τ	ΔQ	Q_o	τ	
34	0.8	5.6-07	7.7-07	1.2-06	2.8-08	150	2.1-06	1.7-08	250			
40	2.7	2.2-07										
45	0.5	9.0-07	2.2-08	3.6-07			4.2-07	3.6-09	200	1.6-06	4.0-09	600
68	0.8	4.3-07										
70	1.3	2.4-06							200			
81	0.2	4.0-06										
110	0.9	4.5-06	2.6-07	4.5-07	1.0-08	50	5.6-07	4.5-09	200			
235	0.8	1.6-06										
350	2.3	9.0-07										
360	3.9	8.0-06										
450	0.9	5.0-06								6.6-07	2.0-09	400
500	0.5	5.0-06										
680	0.2	6.0-07	2.1-07	3.7-07	1.0-09	50	2.6-07					
1,250	0.5	5.0-06										
1,500	2.4	4.8-07										
1,700	3.9	5.2-06										
2,100	1.0	1.0-06	1.0-06	6.4-07	1.6-08	50	5.7-07	5.0-09	200	8.7-07	2.5-09	400
2,200	0.9	6.0-06										
5,500	1.0	4.4-07	2.6-07	2.9-07	6.8-09	60		2.3-09	250			
11,000	3.9	6.5-06										
11,000	3.5	4.6-07										

Table H-11
MICA (2 - .01 μ F, W.V. 600)

Dose [rads(Si)]	Pulse Width (μ sec)	Q_p	ΔQ_{30}	ΔQ	30-100 μ sec Q_0	τ	100-300 μ sec τ	τ
38	3.7	1.0-06	4.0-07	8.1-07	1.6-06	120	7.6-09	150
42	0.4	1.0-06						
50	0.1	8.0-07						
50	1.4	1.2-06						
70	1.3	3.0-06						
80	0.2	4.0-06						
110	0.9	4.0-06						
120	1.4	1.6-06						
155	0.4	9.2-07						
164	1.35	8.4-07	2.5-07	5.7-07	1.2-08	90	5.1-09	140
180	0.3	1.0-06						
326	3.7	1.0-06	2.7-07	6.2-07	1.2-08	106	7.6-09	160
410	3.7	1.2-06	2.5-07	5.1-07	1.0-08	97	5.4-09	140
420	0.1	8.4-07						
450	0.9	3.5-06						
460	0.4	7.5-07						
500	0.5	3.0-06						
820	1.3	1.0-06	2.7-07	2.4-07				
920	0.4	8.0-07						
1,250	0.5	5.0-06						
1,760	3.7	1.2-06	2.0-07	4.1-07				
1,800	1.1	1.2-06						
2,200	3.7	1.2-06	5.6-07					
2,300	0.9	6.0-06						
2,700	1.1	6.2-07	2.3-07					
4,000	1.1	8.4-07						
4,800	0.95	8.6-07	4.1-07					
11,000	3.9	4.7-06						
16,800	3.9	9.0-07	3.8-07	9.4-08	4.5-09	50		
22,000	4.0	1.2-06	4.8-07	1.0-07	1.0-08	20		

NOTE: Values of Q are for 45V applied. Add -20% or +20% for 90V and 22V, respectively.

REFERENCES

1. Radiation Effects Information Center (REIC) Report No. 36, Battelle Memorial Institute, Columbus, Ohio (October 1, 1964).
2. Nichols, D. K., and V. A. J. van Lint, "Theory of Transient Electrical Effects in Irradiated Insulators," IEEE Transactions on Nuclear Science, Vol. NS-13, No. 6 (December 1966).
3. DeMichele, D. W., D. K. Nichols, and V. A. J. van Lint, "Radiation Effects on Dielectric Materials," ECOM-01412-3, GA-7066, Quarterly Report No. 3, DA-28-043-AMC-01412(E), 52 pp, Avail. DDC, AD486668 (July 1966).
4. van Lint, V. A. J., J. W. Harrity, and T. M. Flanagan, "Scaling Laws for Ionization Effects in Insulators," IEEE Transactions on Nuclear Science, Vol. NS-15, No. 6 (December 1968).
5. Rose, Albert, "An Outline of Some Photoconductive Processes," RCA Review, Vol. 12, pp. 362-414 (September 1951).
6. Frankovsky, F. A., and M. Shatzkes, "Reactor and Linear Accelerator Induced Effects in Dielectrics," IBM Corporation, Owego, New York, IBM File No. 65-825-1944.
7. van Lint, V. A. J., R. F. Overmyer, and D. K. Nichols, "Transient Radiation Effects on Electronic Parts," General Dynamics Corporation, General Atomic Division, San Diego, California, GA-6534 (July 10, 1965). Final Report June 16, 1964-June 14, 1965, DA-36-039-SC-89196, 78 pp.
8. Boczar, P. G., G. E. Boyd, W. A. Cardwell, and F. A. Frankovsky, "Study of Effect of High Intensity Pulsed Nuclear Radiation on Electronic Parts and Materials." Final Report on Contract DA28-043-AMC-00212(E), ECOM-00212-F, October 1966.